Electromagnetic interference shielding in X band with aero-GaN

Electromagnetic interference shielding in X-band with aero-GaN

Mircea Dragoman[1], Tudor Braniste[2], Sergiu Iordanescu[1], Martino Aldrigo[1], Simion Raevschi[3], Sindu Shree[4], Rainer Adelung[4], Ion Tiginyanu[2,5*]

[1]*National Research and Development Institute in Microtechnology, Str. Erou Iancu Nicolae 126A, Bucharest 077190, Romania*

[2]*National Center for Materials Study and Testing, Technical University of Moldova, Stefan cel Mare av. 168, Chisinau 2004, Moldova*

[3]*Department of Physics and Engineering, State University of Moldova, Alexei Mateevici str. 60, Chisinau 2009, Moldova*

[4]*Institute for Materials Science, Kiel University, Kaiserstr. 2, Kiel 24143, Germany*

[5]*Academy of Sciences of Moldova, Stefan cel Mare av. 1, Chisinau 2004, Moldova*

We investigate the electromagnetic shielding properties of an ultra-porous lightweight nanomaterial named aerogalnite or simply aero-GaN. Aerogalnite is made of randomly arranged hollow GaN microtetrapods, which were obtained by direct growth using hydride vapour phase epitaxy of GaN on the sacrificial network of ZnO microtetrapods. A 2-mm thick aerogalnite sample exhibits electromagnetic shielding properties in the X-band similar to solid structures based on metal foams or carbon nanomaterials and having the weight lower with 4-5 orders of magnitude the weight of metals.

Corresponding author email: mircea.dragoman@imt.ro

1. Introduction

Electromagnetic interference shielding (EMI) is a crucial issue, since many devices emit electromagnetic (EM) waves and thus have detrimental effects on computers, cell phones, wireless internet and very sensitive equipment such as navigation systems. The reduction of EMI and radar-cross section becomes critical when dealing with millions of small objects which are interconnected by high-frequency EM fields, as in the case of Internet-of-Things (IoT). Much lighter EMI materials are required for many applications, especially in the domains of automotive and aerospace.

The X-band is one of the most important EM bands (8.2-12.4 GHz), since the majority of radars are working in this band, and it is also allocated for terrestrial and space communications. Even traffic light motion sensors and the RF sources of particle accelerators are working in this frequency range. Therefore, the EMI is of outmost importance in X-band and different lightweight materials have been investigated for EMI shielding such as conducting polymers, graphene, carbon nanotubes and nanocomposites based on them [1]. The search for new EMI shielding materials has been lasting for at least two decades and microwave absorbers have been studied using carbon nanotubes (CNTs) in X-band [2], CNT-based composites [3], carbon nanotube networks [4] and doped carbon nanotubes [5]. A recent review about CNT composites for EMI is found in [6]. Lightweight graphene foam composites have emerged as a strong EMI material candidate in X-band due to their low densities of 0.06 g/cm^3, which is twenty times smaller than that inherent to polymer composites [7]. Even lower densities of 0.008 g/cm^3 and very good EMI shielding are obtained with the help of graphene foams and polymer composites [8]. Very good EMI shielding is obtained with reduced graphene oxides (rGO), graphene papers and graphene nanohybrids, these results being reviewed in [9].

The development of 2D atomically thin systems has provided new materials for EMI shielding with performances similar to those of carbon-based nanomaterials, such as MXenes – for example metal carbide and nitrides [10]. Other 2D materials such as MoS_2 nanosheets are used for EMI shielding in combination with rGO [11] and other nanomaterials. The authors of all these references are currently studying EMI shielding in X-band, validating again the urgent need for lightweight materials in this frequency band, driving to important cost reductions of many equipment used in everyday life or in military applications.

Another research branch involves nitride nanocomposites, such as TiN/C [12], nanosized TiN powders [13], Ni3N/Ni [14] and Fe2Ni2N/SiO2 [15], which have been exploited as dielectric /magnetic EM microwave absorbers. In particular, the focus of all these works is on the measure of the microwave absorbance capacity, based on the extraction of the complex permittivity/permeability and on the measurement of the reflection loss, which depends on the dielectric/magnetic loss tangent of the material.

In this paper, we investigate the EMI properties of the the aerogalnite (further termed as aero-GaN) which is a new ultraporous semiconductor nanomaterial formed by hollow GaN micro-tetrapods (with the wall thickness in the nanometer scale) which are interconnected between them; the fabrication method and its physical properties are described in detail in [16]. and will not be repeated here

We will show that aero-GaN has an average conductivity around 10^3 S/m in X-band, low absorption and a good electromagnetic shielding effectiveness which is comparable or even higher with many nanocomposites studied in the literature metioned above.

2. Results and discussions

The total EM shielding effectiveness (SE) is given by:

$$SE(dB) = SE_R(dB) + SE_A(dB) \quad (1)$$

where SE_R is the shielding effectiveness due to EM reflections and SE_A is the shielding effectiveness due to absorption. The above formula entails that there are two basic physical mechanisms to obtain high *SE*: (i) high EM reflection, specific for metals with high conductivity of about 10^7 S/m and very low absorption in X-band; (ii) high absorption in X-band and conductivity as low as tens of S/m inherent to composites such as graphene foams. *SE* cannot be tuned in the case of metals, while *SE* is tunable in the case of composites by varying the concentration of their constituents.

In Fig. 1, we have depicted the scanning electron microscopy (SEM) images of the aero-GaN and the optical image of the samples. The dimensions of the samples are 24x12x2 mm^3 and they were fabricated with two different porosities (thus, with two different densities), i.e. 97% and 98.5% of porosity, having the densities 0.185 g/cm^3 and 0.089 g/cm^3, further referred to as GaN2 and GaN1, respectively.

The EMI shielding effect of aero-GaN samples has been measured with a calibrated VNA (Vector Network Analyzer) connected to a X-band waveguide-based set-up, as indicated in Fig. 2 and the S-parameters at the two ports have been measured providing the reflection and transmission coefficients at each port (S_{11} and S_{22} are the reflection parameters at the two ports, whereas S_{21} and S_{12} are the transmission parameters between the two ports). The measured S-parameters of the aero-GaN samples with different porosities are represented in Fig. 3. We have represented only S_{11} and S_{21}, since S_{22} is identical with S_{11}, and S_{12} with S_{21} (due to reciprocity and symmetry of the scattering matrix, which is typical for measurements of passive components). We see that in the absence of aero-GaN we have an almost perfect transmission of EM waves inside the waveguide, while when aero-GaN is introduced strong reflections appear in the waveguide and the transmission is decreasing dramatically. For example, at 10 GHz the transmission decreases from less than -0.2 dB to -15 dB and -20 dB, respectively, for the two different porosities of aero-GaN explored in this work.

Using the measured S-parameters, we can extract *SE*, SE_R and SE_A which are represented in Fig. 4 for the two aero-GaN porosities. In detail, we have:

$$SE(dB) = SE_R(dB) + SE_A(dB) = 10\log[(1/(1-|S11|_2) + 10\log[(1-|S_{11}|^2 / |S_{21}|^2] \qquad (2)$$

From the experimental results we see that decreasing slightly the porosity, which entails an increasing in the number of conductive GaN tetrapods and their interconnections, the conductivity increases more than one order of magnitude; this way, from Fig. 4 we can observe an *SE* of about 14.5±2 dB for the GaN1 sample, and an *SE* of 25±2 dB for the GaN2 sample over the X-band. Since SE_R = 39.5+10log($\sigma/2\pi f\mu$) where σ is the electric conductivity and μ is the relative magnetic permeability (considered equal to 1), we can extract the conductivity of aero-GaN in X-band depicted in Fig. 5 for the two porosities. Accordingly, the maximum σ is about 240 S/m for the GaN1 sample and about 1700 S/m for the GaN2 sample. If we compare these results to those of table S2 in supplementary materials in Ref.10, it is evident that the aero-GaN has a conductivity of the same order of magnitude of Ni-Co fiber in wax matrix [17], or of Ag nanowires in PS matrix [18].

Considering the results obtained for the GaN1 sample, its maximum specific *SE* given by *SSE* = *SE*/ρ (where ρ is the density in g/cm^3) is 185 dBcm^3/g, hence comparable with many carbon composites and solid structures based on metal foams, metal fibers and metal filaments embedded in polymer matrix composites (see table S3 in supplementary materials in Ref.10). For example, for carbon-based foam structures *SSE* is between 33 dBcm^3/g (SWCNT foam [19]) and 937 dBcm^3/g (rGO, 26 wt.% [20]), whereas GaN1 exhibits superior performance with respect to some metal-based foams (CuNi [21] and SS [22]). However, carbon-based foams are brittle materials, difficult to be fabricated in the form of thin and even thick films with rather large dimensions. From the same table, one can see that considering solid structures, GaN1 exhibits almost in all case a specific shielding performance which is one order of magnitude greater than all carbon-based, metal-based and MXenes materials.

3. Conclusions.

In this work, we have demonstrated that aero-GaN is an EMI shielding material with good performances in X-band. We point out that the aero-GaN samples are able to cover an entire monolithic microwave integrated circuit (MMIC), which has overall dimensions smaller than or comparable to our samples, depending on its application and output power. For example, our aero-GaN samples have the area of 288 mm^2, while the surface of an advanced MMIC T/R module dedicated to space borne radar in X-band and made of two stages power amplifier, three-stage low noise amplifier and MMIC SPDT switches has a total area of 230 mm^2 [23].

Acknowledgments

T.B. and I.T. acknowledge the support from the Ministry of Education, Culture and Research of the Republic of Moldova under the Grant #15.817.02.29A, as well as from the European Commission under the Grant #810652 “NanoMedTwin”. S.S. and R.A. acknowledge the support by the Deutsche Forschungsgemeinschaft (DFG) in the framework of SFB 677 project C-14 and SFB 1261 project A5. M.D, M.A, and S.I.

acknowledge the financial support of project number PN-III-P4-ID-PCCF-2016-0033.

References

[1] P. Saini, and M. Arora, Microwave absorption and EMI shielding behavior of nanocomposites based on intrinsically conducting polymers, graphene and carbon nanotubes, in *New Polymers for Special Applications*, Ailton De Souza Gomes (Ed.), Ch. 3, Intech, London, 2012

[2] P. C. P. Watts, W.-K. Hsu, A. Barnes, and B. Chambers, High-permittivity of defective carbon nanotubes in X-band, Adv. Materials **15,** 600–603 (2003)

[3] B. Wen, M.-S. Cao, Z.-L. Hou, W.-L. Song, L. Zhang, M.-M. Lu, H.-B. Jin, X.-Y. Fang, W.-Z. Wang, J. Yuan, Temperature dependent microwave attenuation behavior for carbon-nanotube/silica composites, Carbon 65, 124–139 (2013)

[4] B. De Vivo, P. Lamberti, G. Spinelli, and V. Tucci, A morphological and structural approach to evaluate the electromagnetic performances of composites based on random networks of carbon nanotubes, Journal of Applied Physics **115**, 154311 (2014)

[5] Z. Wang, G. Wei, and G.-L. Zhao, Enhanced electromagnetic wave shielding effectiveness of Fe doped carbon nanotubes/epoxy composites wave shielding effectiveness of Fe doped carbon nanotubes/epoxy composites, Appl. Phys. Lett. **103**, 183109 (2013)

[6] M. González, G. Mokry, M. de Nicolás, J. Baselga, and J. Pozuelo, Carbon nanotube composites as electromagnetic shielding materials in GHz range in carbon nanotubes, in *Carbon Nanotubes*, M. Berber and I. Hazzaa Hafez, Intech, London, 2016

[7] Z. Chen, C. Xu, C. Ma, W. Ren, and H.-M. Cheng, Lightweight and flexible graphene foam composites for high-performance electromagnetic interference shielding, Adv. Mater.,

25, 1296–1300 (2013)

[8] Y. Wu, Z. Wang, X. Liu, X. Shen, Q. Zheng, Q. Xue, and J.-K. Kim, Ultralight graphene foam/conductive polymer composites for exceptional electromagnetic interference shielding, ACS Appl. Mater. Interfaces **9**, 9059–9069 (2017)

[9] M. Cao, C. Han, X. Wang, M. Zhang, Y. Zhang, J. Shu, H. Yang, X. Fang, and J. Yuan, Graphene nanohybrids: excellent electromagnetic properties for the absorbing and shielding of electromagnetic waves, J. Mater. Chem. C, **6**, 4586–4602 (2018)

[10] F. Shahzad, M. Alhabeb, C. B. Hatter, B. Anasori, S. M. Hong, C. M. Koo, and Y. Gogotsi, Electromagnetic interference shielding with 2D transition metal carbides (MXenes), Science **353**, 1137–1140 (2016)

[11] M. Ning, B. Kuang, Z. Hou, L. Wang, J. Li, Y. Zhao, and H. Jin, Layer by layer 2D MoS_2/rGO hybrids: An optimized microwave absorber for high-efficient microwave absorption, Applied Surface Science **470**, 899–907 (2019)

[12] Y. Wei. L. Zhang, C. Gong, S. Liu, M. Zhang, Y. Shi, and J. Zhang, Fabrication of TiN/Carbon nanofibers by electrospinning and their electromagnetic wave absorption properties, Journal of Alloys and Compounds **735**, 1488–1493 (2018)

[13] C. Gong, J. Zhang, C. Yan, X. Cheng, J. Zhang, L. Yu, Z. Jin, and Z. Zhang, Synthesis and microwave electromagnetic properties of nanosized titanium nitride, Journal ofMaterials Chemistry **22**, 3370–3376 (2012)

[14] C. Gong, Y. Jia, X. Zhao, Ha. Liu, X. Lv, L. Yu, J. Zhang, and J. Zhou, Ni3N/Ni composites with in-situ growth heterogeneous interfaces as microwave absorbing materials, Appl. Phys. Lett. **107**, 153905 (2015)

[15] H. Pan, X. Cheng, C. Zhang, C. Gong, L. Yu, J. Zhang, and Z. Zhang, Preparation of Fe2Ni2N/SiO2 nanocomposite via a two-step route and investigation of its electromagnetic

properties, Appl. Phys. Lett. **102**, 012410 (2013)

[16] I. Tiginyanu, T. Braniste, D. Smazna, M. Deng, F. Schütt, A. Schuchardt, M. A. Stevens-Kalceff, S. Raevschi, U. Schürmann, L. Kienle, N. M. Pugno, Y. K. Mishra, and R. Adelung, Self-organized and self-propelled aero-GaN with dual hydrophilic-hydrophobic behaviour, Nano Energy **56,** 759–769 (2019)

[17] X. Huang, B. Dai, Y. Ren, J. Xu, and P. Zhu, Preparation and study of electromagnetic interference shielding materials comprised of ni-co coated on web-like biocarbon nanofibers via electroless deposition, J. Nanomater. 2015, 320306 (2015)

[18] M. Arjmand, A. A. Moud, Y. Li, U. Sundararaj, Outstanding electromagnetic interference shielding of silver nanowires: Comparison with carbon nanotubes, RSC Adv. **5**, 56590–56598 (2015)

[19] Y. Yang, M. C. Gupta, K. L. Dudley, and R. W. Lawrence, Novel carbon nanotube-polystyrene foam composites for electromagnetic interference shielding, Nano Lett. **5**, 2131–2134

[20] Y. Li, X. Pei, B. Shen, W. Zhai, L. Zhang, W. Zheng, Polyimide/graphene composite foam sheets with ultrahigh thermostability for electromagnetic interference shielding, RSC Adv. **5**, 24342–24351 (2015)

[21] K. Ji, H. Zhao, J. Zhang, J. Chen, Z. Dai, Fabrication and electromagnetic interference shielding performance of open-cell foam of a Cu–Ni alloy integrated with CNTs, Appl. Surf. Sci. **311**, 351–356 (2014)

[22] A. Ameli, M. Nofar, S. Wang, C.B. Park, Lightweight polypropylene/stainless-steel fiber composite foams with low percolation for efficient electromagnetic interference shielding, ACS Appl. Mater. Interfaces **6**, 11091–11100 (2014)

[23] S. D'Angelo, A. Biondi, F. Scappaviva, D. Resca, and V. A. Monaco, A GaN MMIC

chipset suitable for integration in future X-band spaceborne radar T/R module frontends, 2016 21st International Conference on Microwave, Radar and Wireless Communications (MIKON), Krakow, Poland, doi: 10.1109/MIKON.2016.7492014

Figure Captions

Fig. 1. (a) and (b): SEM images of aero-GaN; (c) an optical image of a representative sample used for RF measurements.

Fig. 2. Schematics of the RF measurement set-up. The S-parameters are normalized on the standard characteristic impedance of 50 Ω.

Fig. 3. S-parameter measurement of samples having two porosities denoted as GaN1 and GaN2: (a) return loss (S_{11}) and (b) transmission (S_{21}) for GaN1 (blue triangles) and GaN2 (red squares). The reference case of waveguide without sample is represented by the black rhombi.

Fig. 4. Total shielding effectiveness (*SE*, black rhombi), reflection shieding effectiveness (SE_R, red squares) and absorption shielding effectiveness (SE_A, blue triangles) for the two aero-GaN porosities: (a) GaN1 and (b) GaN2.

Fig. 5. Conductivity in X-band of the aero-GaN samples with different degree of porosity: GaN1 (blue triangles) and GaN2 (red squares).

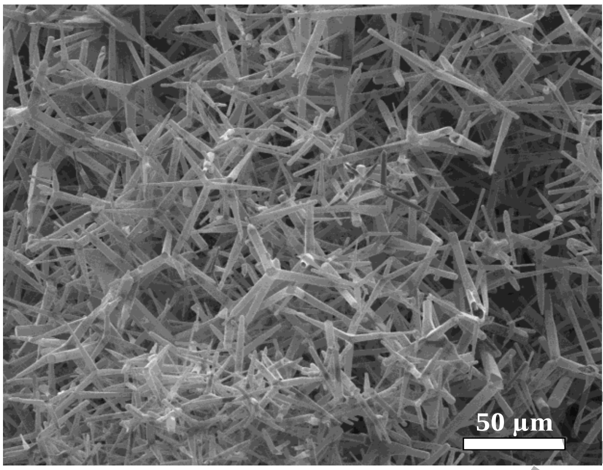

(a)

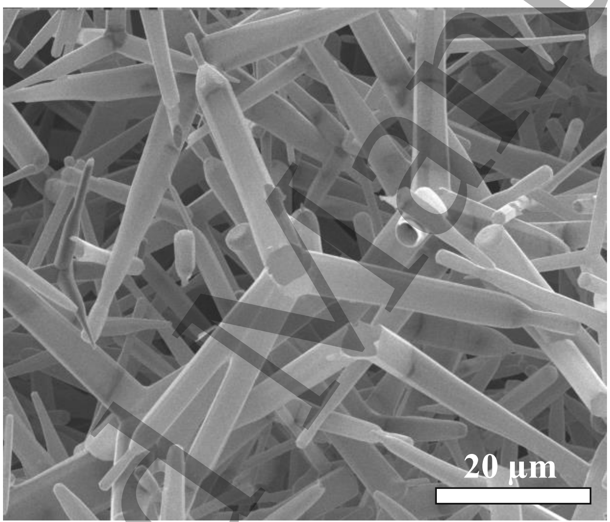

(b)

(c)

Fig. 1

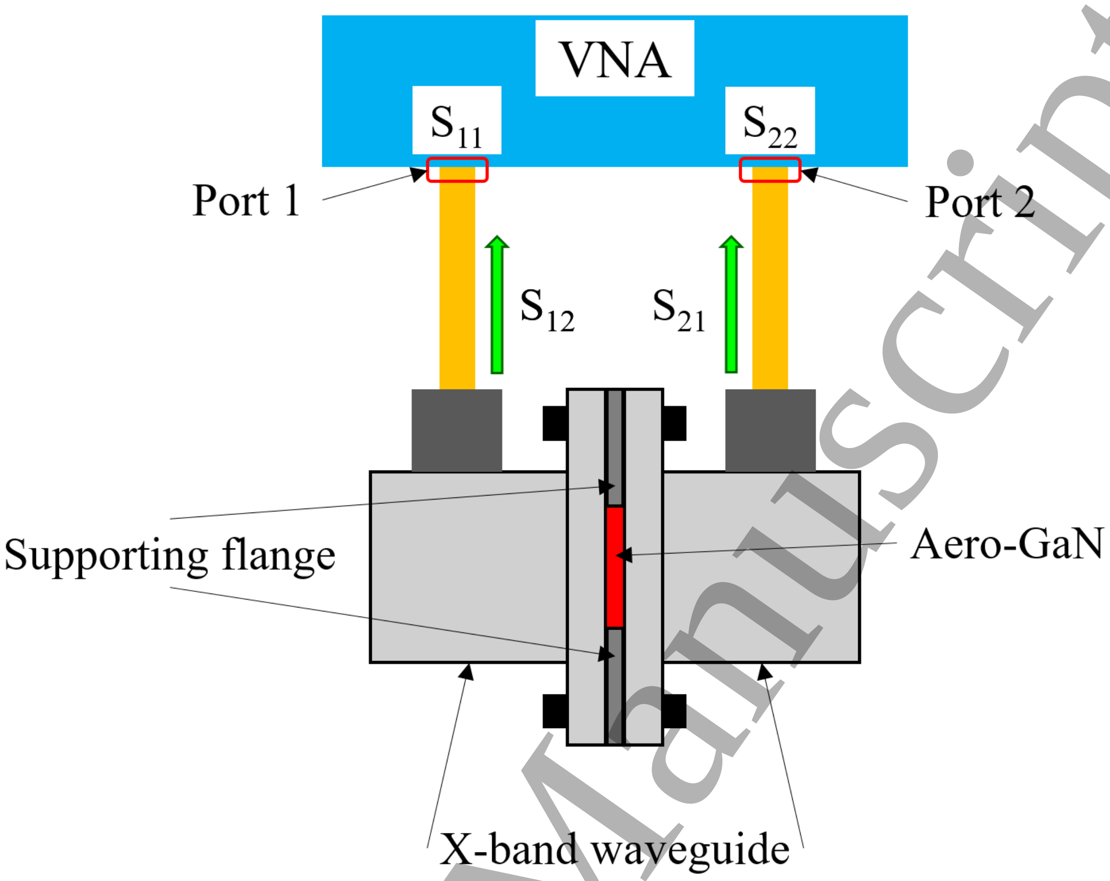
VNA
S11
S22
Port 1
Port 2
S12
S21
Supporting flange
Aero-GaN
X-band waveguide

Fig. 2

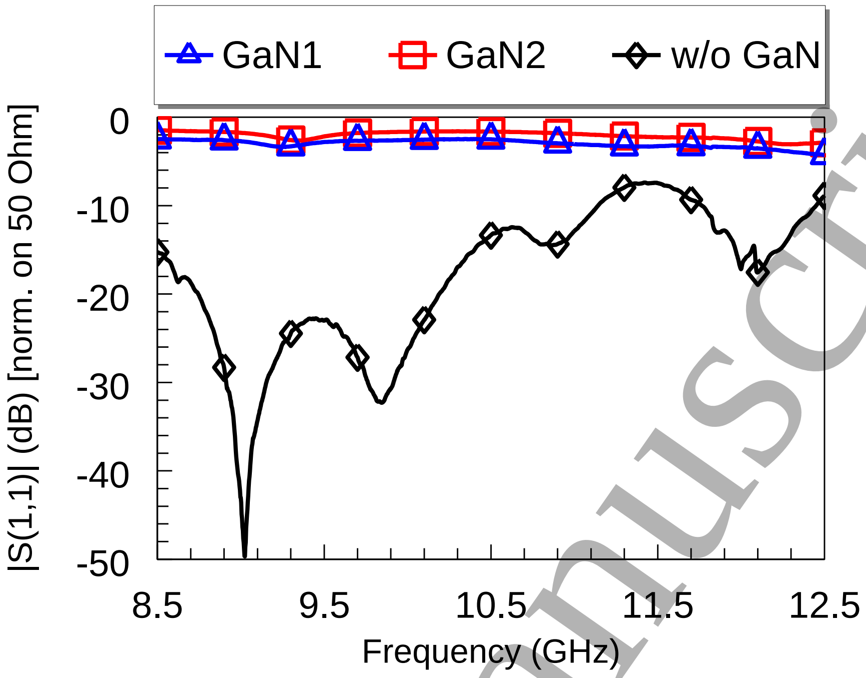
GaN1
GaN2
w/o GaN
|S(1,1)| (dB) [norm. on 50 Ohm]
0
-10
-20
-30
-40
-50
8.5
9.5
10.5
11.5
12.5
Frequency (GHz)

(a)

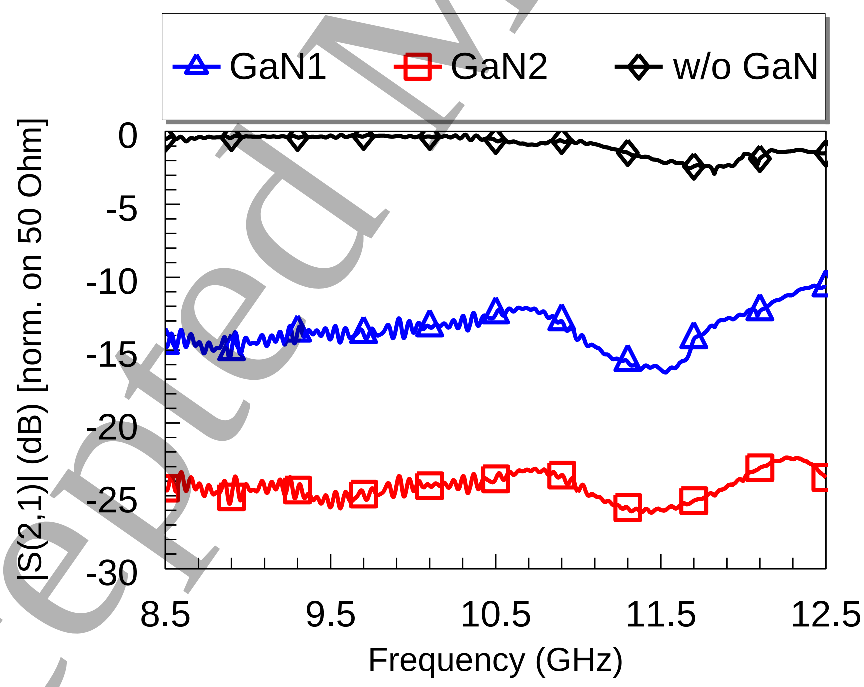
GaN1
GaN2
w/o GaN
|S(2,1)| (dB) [norm. on 50 Ohm]
0
-5
-10
-15
-20
-25
-30
8.5
9.5
10.5
11.5
12.5
Frequency (GHz)

(b)

Fig. 3

14

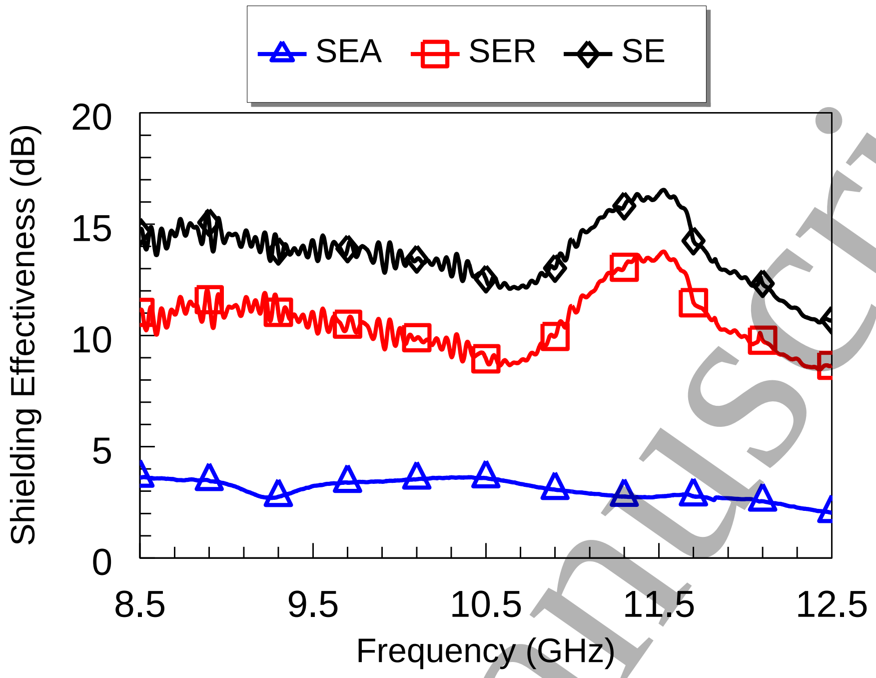
SEA
SER
SE
Shielding Effectiveness (dB)
20
15
10
5
0
8.5
9.5
10.5
11.5
12.5
Frequency (GHz)

(a)

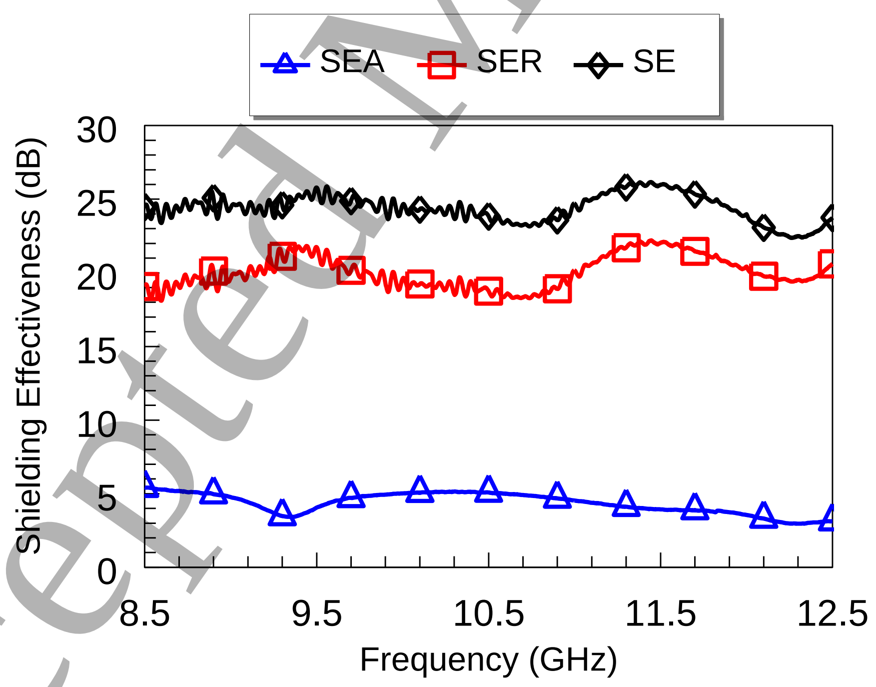
SEA
SER
SE
Shielding Effectiveness (dB)
30
25
20
15
10
5
0
8.5
9.5
10.5
11.5
12.5
Frequency (GHz)

(b)

Fig. 4

15

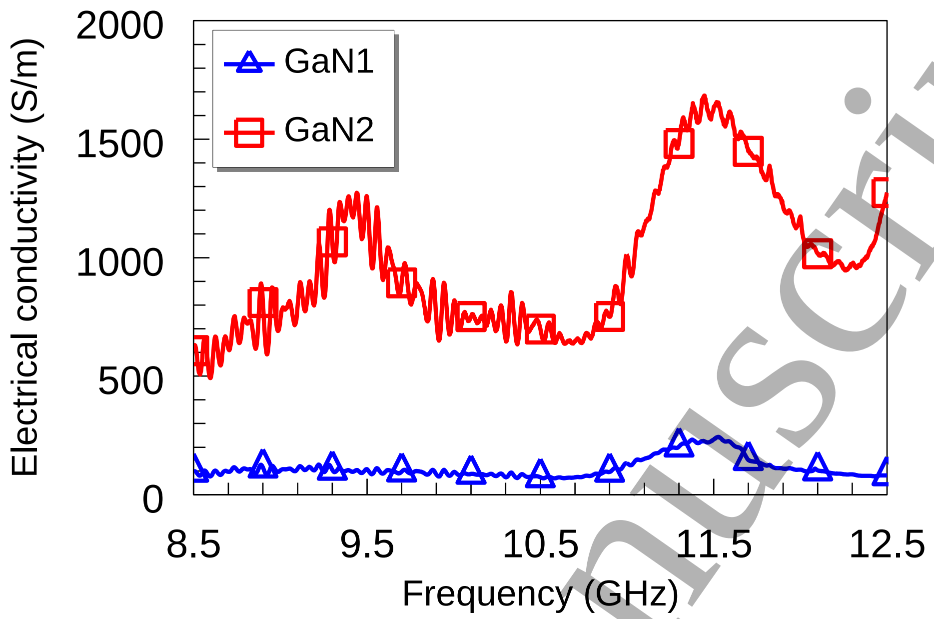
GaN1
GaN2
Electrical conductivity (S/m)
Frequency (GHz)
2000
1500
1000
500
0
8.5
9.5
10.5
11.5
12.5

Fig. 5